



Application of zeolite prepared from natural materials for reducing ground water salinity and sodium ion from Wadi El-Assiuti

Ahmed A. Abdelmoneim^a, Mohamed Abdul-Moneim^b, Ahmed A. Geies^c,
Seham O. Farghaly^{a,*}

^aGeology Departments, Faculty of Science, Sohag University, Sohag, Egypt, email: seham.omran3120@yahoo.com (S.O. Farghaly)

^bGeology Department, Faculty of Science, Assiut University, Assiut, 71516, Egypt

^cChemistry Department, Faculty of Science, Assiut University, Assiut, 71516, Egypt

Received 6 December 2019; Accepted 12 February 2020

ABSTRACT

Groundwater is an important source of freshwater in Egypt. With growing populations and human activities in Egypt, the demand for groundwater has increased. In this study, sodalite was successfully synthesized from low-cost natural clay materials (kaoline) and white sand using the fusion with the NaOH method. The conditions of hydrothermal crystallization (zeolitization) were found at a temperature of 170°C, and a time span of 72 h for raw material. Sodalite has been characterized by X-ray diffraction, scanning electron microscopy, Fourier transform infrared spectroscopy, and differential thermal analysis/thermogravimetric analysis. Sodalite was tested as adsorbents for reducing a variety of salinity total dissolved solids with Na cation from groundwater of Wadi El-Assiuti, Egypt. Batch experiments were carried out to investigate the effects of some parameters (dosage of adsorbent, pH, temperature, and contact time) on both salinity and the Na⁺ ion adsorption. The results showed that sodalite has a good efficiency in the removal of salinity and the Na⁺ ion with concentrations up to 6,000 and 1,320 ppm respectively. The percent adsorption was evaluated with changes in the previous parameters for different concentrations of Na⁺ ion. The Langmuir constants model for Na⁺ ion sorption on the adsorption isotherms is fitted well. The R_L value in the present investigation at concentration 1,320 ppm was less than one, indicating that the adsorption of the metal ion by sodalite is favorable. Freundlich adsorption isotherm is also adapted in the case of sodalite ($R^2 = 0.7$) for Na⁺ ion.

Keywords: Sodalite; Kaoline (sand); Hydrothermal reactions; Zeolite; Clay; Groundwater; Characterization; Element contents; Water treatment

1. Introduction

Groundwater is an important source of freshwater stored in aquifers. Aquifers are permeable, pervious, and porous rocks with connected pore spaces that allow water to flow through them. Aquifers can either be confined or unconfined. Depending on the rock type and formation, groundwater is found in the ground within the depth of 100 m and in some places up to 1,000 m deep. Groundwater quality assessment examines “the chemical, biological and physical qualities of the water”, including temperature,

turbidity, color, taste, and odor [1]. But the major concerns are usually with the chemical and biological parameters and their health implication on the environment. A great percentage of people worldwide use this source of water for their agricultural, domestic, and industrial purposes [2]. Variation in groundwater chemistry is mainly a function of the interaction between the groundwater and the mineral composition of the aquifer materials through which it moves. Hydrochemical processes, including dissolution, precipitation, ion exchange, sorption, and desorption, together with the residence time occurring along the flow

* Corresponding author.

Presented at the 4th International Water Desalination Conference: Future of Water Desalination in Egypt and the Middle East, 24–27 February 2020, Cairo, Egypt

1944-3994/1944-3986 © 2020 Desalination Publications. All rights reserved.

path, control the variation in the chemical composition of groundwater [3].

Salinity is a term used to describe the amount of salt in a given water sample. It usually is referred to in terms of total dissolved solids (TDS) and is measured in milligrams of solids per liter (mg/L). Water with a TDS concentration greater than 1,000 mg/L commonly is considered saline. This somewhat arbitrary upper limit of freshwater is based on the suitability of water for human consumption. Although water with TDS greater than 1,000 mg/L is used for domestic supply in areas where the water of lower TDS content is not available, water containing more than 3,000 mg/L is generally too salty to drink. [4]. Desalination is a water treatment process that removes salts from water. Desalination presents the possibility of providing freshwater not only from the ocean but also from saline groundwater. "By 2020, desalination and water purification technologies will contribute significantly to ensuring a safe, sustainable, affordable, and adequate water supply for our nation." [2].

Various technologies have been used to remove TDS from groundwater, including reverse osmosis, ultrafiltration, ion exchange, ion-exchange-membrane bioreactors, catalytic reduction, electro dialysis, activated carbon, land disposal, chemical denitrification, and microbiological treatment [5–7]. Sodium (Na^+) is the most important and abundant of the alkali metals in natural waters to which the salinity of the groundwater is directly related. Sources of sodium (Na^+) are halite (NaCl), sea spray, hot springs, brines, and some silicates or rare minerals such as nahcolite (NaHCO_3). In groundwater source of sodium content is greatly dependent on the rock type of aquifer. Its concentration of more than 50 ppm makes the water salt taste and causes health problems it may affect the taste of drinking water at levels above 200 ppm [8].

Zeolites are crystalline hydrated aluminum silicates with a framework structure containing pores that are occupied by water and by alkali and alkaline earth cations. [9]. The structures of zeolites consist of three-dimensional frameworks of SiO_4 and AlO_4 tetrahedra. The aluminum ion is small enough to occupy the position in the center of the tetrahedron of four oxygen atoms, and the isomorphous replacement of Si^{4+} by Al^{3+} produces a negative charge in the lattice. The net negative charge is balanced by the exchangeable cation (sodium, potassium, or calcium). [10]. These cations are exchangeable with certain cations in solutions such as lead, cadmium, zinc, and manganese. The fact that zeolite exchangeable ions are relatively innocuous (sodium, calcium, and potassium ions) makes them particularly suitable for removing undesirable heavy metal ions from industrial effluent waters. [9].

Sodalite, is a rich royal blue tectosilicates mineral $[\text{Na}_4(\text{AlSi}_3\text{O}_8)_2\text{Cl}]_2$, can be defined as a crystalline microporous material whose structure is characterized by a tetrahedral network displaying enclosing voids of at least 2.5 Å in diameter. The extreme similarity of sodalite with low silica zeolitic minerals (i.e., Na-X, Na-P, Na-A zeolites) justifies the great interest in sodalite synthesis processes, carried out at industrial scale not only to investigate the crystal structure of the mineral, but especially to explore its properties in environmental fields like wastewater purification through cationic exchange processes, molecules

absorption etc. Sodalite is a rich royal blue tectosilicates mineral widely used as an ornamental gemstone. The aluminosilicate network comprises SiO_4 and AlO_4 tetrahedrons linked by their corners. By virtue of this structure, cubic-octahedral cage units are formed. The chemical formula of sodalite is $(\text{Na}_8[(\text{Al}_6\text{Si}_6\text{O}_{24})]\text{Cl}_2)$ [11]. Generally, zeolite minerals are rare in all of the world, therefore over 200 synthetic zeolites have been synthesized either using chemicals or natural materials. The main objective of this study focused on utilization of the low cost and abundance materials such as clay (kaolinite) and sand for synthetic sodalite and used it to reduce salinity and Na^+ ion from natural groundwater from the Wadi El-Assiuti area.

2. Hydrogeological setting of Wadi El-Assiuti

Wadi El-Assiuti is one of the most notable areas of the Egyptian Eastern Desert. It is the largest and greatest dry valley that runs in the Sahara Desert for a distance of about 115 km. Its area represents a segment of the Nile valley in Upper Egypt. It is located on the fringes of the flood plane east of Assiut city. The area is bounded by latitudes $27^\circ 5' \text{N}$ and $27^\circ 20' \text{N}$ and longitudes $31^\circ 10' \text{E}$ and $31^\circ 25' \text{E}$. The area is located in an arid region with almost no rainfall. Temperature varies from 5°C in winter to 45°C in summer. Several studies were previously carried out in this study area for dealing with its evaluation of its groundwater potential. The study area is a rectangular flat area of about 400 km². It is bounded from the west by the Nile River and from the other sides by the limestone plateau that is dissected by a great number of wadis. [12–15]. Groundwater in this aquifer is characterized by freshwater. The salinity from 800 to 1,000 mg/L. The salt assemblages are: $\text{Ca}(\text{HCO}_3)_2$, $\text{Mg}(\text{HCO}_3)_2$, NaHCO_3 , Na_2SO_4 , and NaCl which indicate a clear resemblance to the salt assemblages of surface water. The study of hydrochemical characteristics in Wadi El-Assiuti revealed on the high concentration of salinity and Na^+ ion in some studied wells relative to [16,17].

3. Methodology

The raw materials that used in sodalite synthesis were natural clay materials (kaoline) and white sand (98 wt.% Si) used as silica source, aluminum solution (4 mg/L) was prepared also as alumina source and distilled water using standard purification methods used in the zeolite as a source of Al and Si. The chemical composition of the raw material kaolinite are given in Table 1.

3.1. Preparation of aluminum solution [18]

- Dissolved 1 g of Al wire in a minimum amount of (1+1) HCL.
- Adding a small drop of mercury as a catalyst.
- Dilute to 1 L with 1% (v/v) HCL.
- Filter the solution to remove the mercury.

3.2. Synthesis of sodalite

Sodalite was synthesized through a hydrothermal method with synthesis conditions. At first, a certain amount of

sodium hydroxide and sand were mixed and was calcinated at 723 K for 4 h. To obtain the final batch gel compositions of $6\text{Na}_2\text{O}:0.75\text{Al}_2\text{O}_3:30\text{SiO}_2:x\text{H}_2\text{O}$ ($x = 710, 780, \text{ and } 850$), deionized water and kaolin were added to the calcinated mixture. The gel was then transferred to a stainless-steel autoclave and stirred on the magnetic stirrer about 1 h after that transferred to the oven and left to crystallize at 448 K for 3 d. The product was recovered by filtration, washed thoroughly with deionized water, and dried at 120°C overnight. The molar gel composition for sodalite synthesis was $(\text{Na}_8[(\text{Al}_6\text{Si}_6\text{O}_{24})]\text{Cl}_2)$. The structure of the synthetic products was studied by methods of X-ray diffraction (XRD), scanning electron microscopy (SEM), FT-IR spectroscopy, and differential thermal analysis/thermal gravimetric analysis (DTA/TGA) and surface area analyzer, the synthetic zeolite was identified and characterized by the next measurements. The X-ray diffract graphs of the raw material and synthetic zeolite were obtained by using XRD pattern, recorded on a Philips Expert (30 mA, 40 kV) with $\text{CuK}\alpha$ radiation. The morphologies of the raw material and synthetic zeolite were

examined by scanning electron microscope (SEM using a Jeol JSM-5400 LV instrument. SEM sample was prepared on a copper holder by placing a smooth part of the zeolite powder and then covered with gold–palladium alloy. SEM images were taken using a Penta Z Z-50P Camera with Ilford film at an accelerating voltage of 15 kV using a low-dose technique., Fourier transform infrared spectroscopy (FT-IR) spectra were recorded on IR-470, infrared spectrophotometer, Shimadzu by using the KBr pellet technique. TGA and differential thermal gravimetric (DTG) were carried out in the air with Shimadzu DTG-60 at a heating rate of $10^\circ\text{C}/\text{min}$.

4. Results and discussion

4.1. Characterization

4.1.1. X-ray diffraction

The identification and characterizations of the raw material and synthetic zeolite shown in Fig. 2 a 2θ range of 5° – 55° . Kaoline is the predominant mineral phase in the raw material which can be identified by its characteristic XRD peaks at 12.34° and 24.64° 2θ (Fig. 2a). However, minor mineral impurities, such as quartz, illite, muscovite, and halloysite, also occur. The X-ray diffractograms of the synthesized given reflection peaks at 2θ , 14.097° , 24.438° , 31.752° , 34.765° , and 42.888° , as shown in the XRD patterns Fig. 2b, which is consistent with that of the reference for sodalite [JCPDS 81-0705] [19].

4.1.2. Scanning electron microscopy

The morphology of the raw material and synthetic zeolite were examined as shown in Figs. 3a and b. The main morphological features observed in the synthesized analcime from met kaolinite are, solid spherical crystallites of SOD and residual met kaolinite (Figs. 3a and b) [20–22].

4.2. FT-IR spectroscopy

The characterization of raw material (kaolinite) and synthetic sodalite with transmission FT-IR is described in Table

Table 1
Chemical composition of kaolinite

| Composition | Content (wt.%) |
|-------------------------|----------------|
| SiO_2 | 49.2 |
| TiO_2 | 2.82 |
| Al_2O_3 | 32.97 |
| Fe_2O_3 | 6.82 |
| MnO | 0.24 |
| MgO | 2.2 |
| CaO | 9.43 |
| Na_2O | 0.8 |
| K_2O | 0.05 |
| P_2O_5 | 0.13 |
| SO_3 | 0.26 |

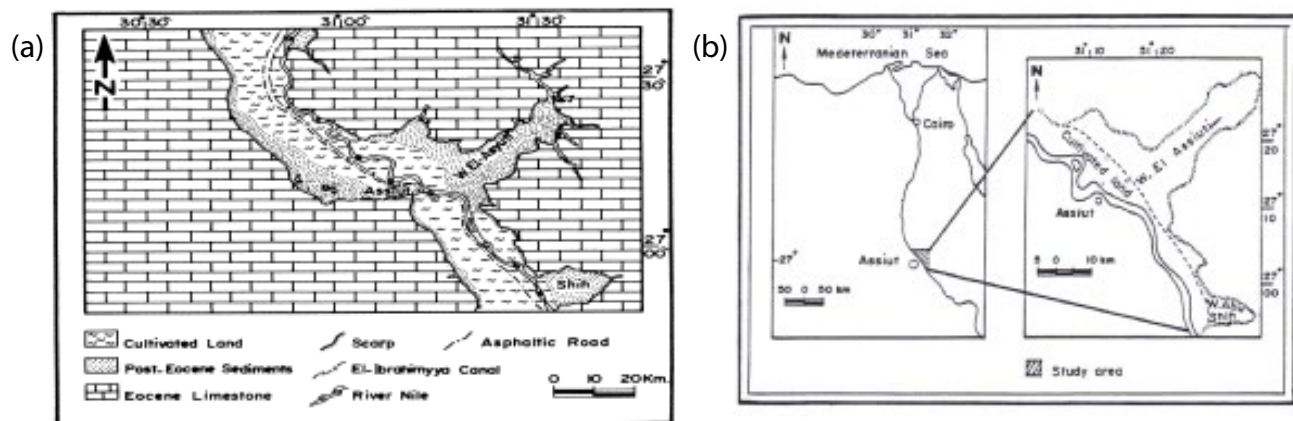


Fig. 1. (a and b). Simplified geological and location map of Wadi El-Assiuti.

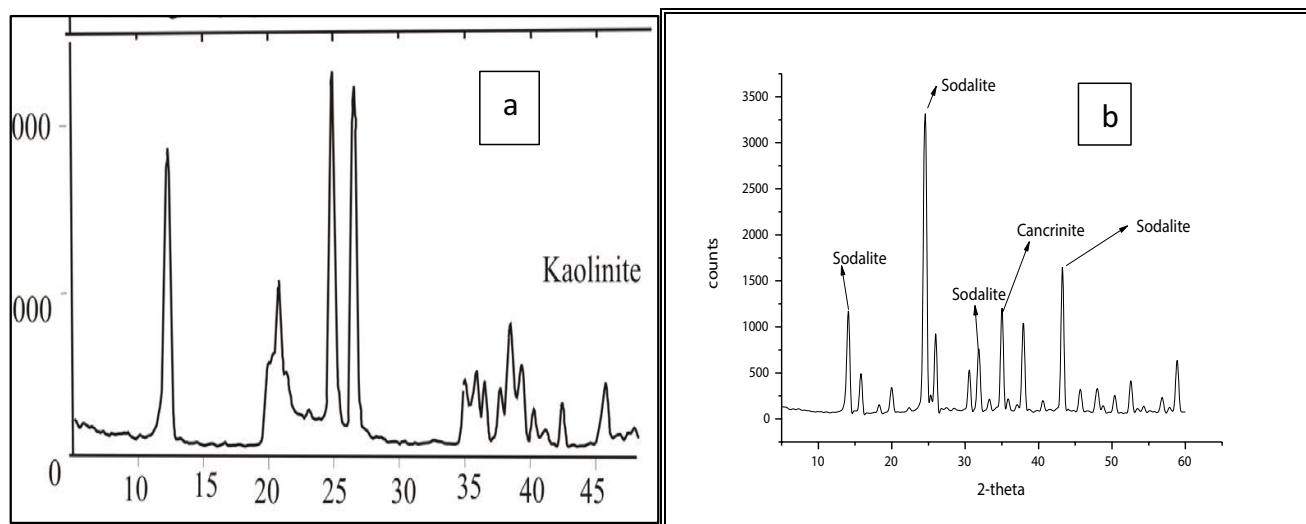


Fig. 2. XRD patterns of (a) raw material kaolinite and (b) synthetic sodalite.

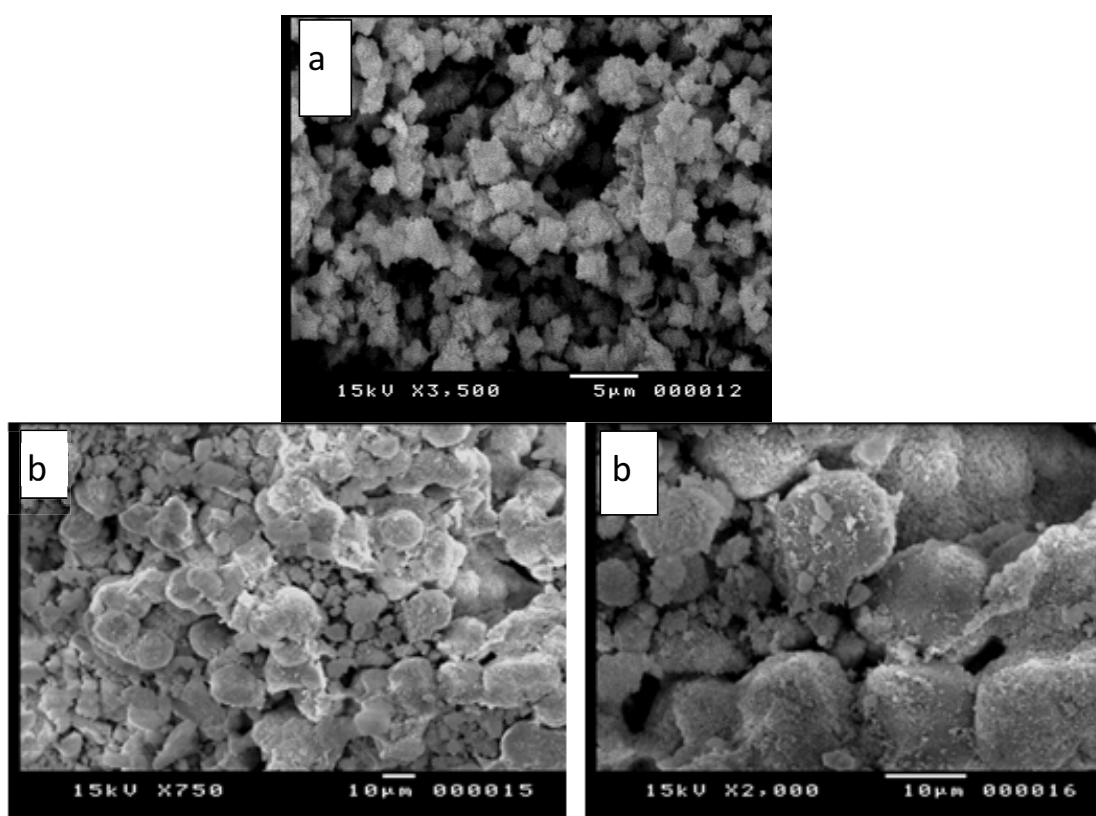


Fig. 3. SEM micrographs of (a) raw material kaolinite and (b) synthetic sodalite.

2, Figs. 4a and b. The characteristic OH-stretching vibrations of kaolinite band at 3460.71 cm^{-1} . The symmetric stretch ($753\text{--}71\text{ cm}^{-1}$), double ring vibration ($63\text{--}44\text{ cm}^{-1}$), T-O bending modes (44.04 cm^{-1}), or the internal linkage vibrations of TO_4 (T = Si or Al) tetrahedral and to symmetrical stretching respectively. The bands at ($1,677.26\text{ cm}^{-1}$) are assigned to the water in the channels of kaoline. FT-IR spectroscopy is used to probe the structure of the synthesized sodalite and

monitor reactions in zeolite pores. Specifically, structural information can be obtained from the vibrational frequencies of the zeolite lattice observed in the range between 200 and $1,500\text{ cm}^{-1}$ [23]. In general, each zeolite has a characteristic infrared pattern. However, some common features are observed which, include the asymmetric ($950\text{--}1,250\text{ cm}^{-1}$) and symmetric stretch ($660\text{--}770\text{ cm}^{-1}$), double ring vibration ($500\text{--}650\text{ cm}^{-1}$), T-O bending modes ($420\text{--}500\text{ cm}^{-1}$), and

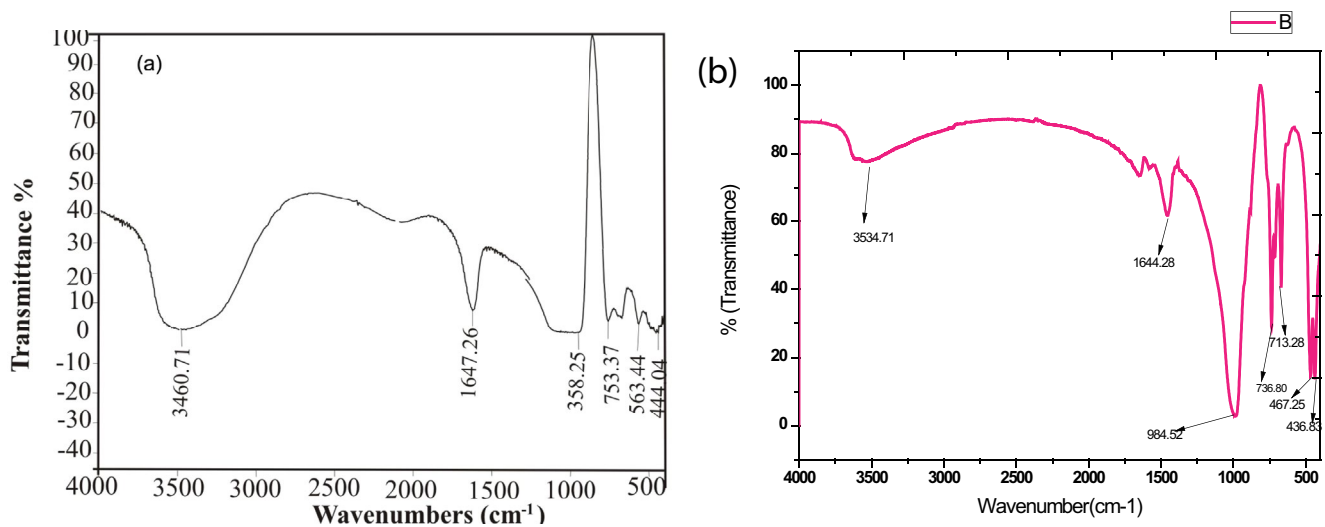


Fig. 4. Fourier transforms infrared spectroscopy (FT-IR) of, (a) raw material kaolinite and (b) synthetic sodalite.

Table 2
Fourier transform infrared (FT-IR) spectroscopy of synthetic sodalite

| | Characteristic band (cm ⁻¹) | Analysis of bands |
|----------|-----------------------------------------|--------------------------------------------------------|
| Sodalite | 3,534.71 (b) | O–H stretching |
| | 1,644.28 (w) | Bending H–O–H |
| | 1,455 (m) | Na–T stretching |
| | 984.52 (m) | Asymmetric Al–O stretch of sodalite |
| | 669.70–736.80 (s) | 4 or 6-membered double rings |
| | 467.25- (s) | Symmetric Al–O stretch of sodalite |
| | 436.83- (s) | Sending vibrations of Si–O and Al–O of the tetrahedral |

possibly opening modes (400–420 cm⁻¹). The FT-IR-spectral data of the synthesized sodalite is presented in (Fig. 4b). The double rings (D4R and D6R) in the framework structures of the zeolitic (500–650 cm⁻¹), is near to 669 (s) cm⁻¹, which is characteristics sodalite, [24]. The bands at 467 (s) cm⁻¹ of sodalite, is near the absorption bands within the range 420–500 cm⁻¹ which are related to the T–O–T bending of vibration mode (T = Al, Si), respectively. These absorption bands characterizing T–O bending vibrations may be shifted to lower frequencies due to decreasing Si/Al ratio in the internal linkage due to the different length of the Al–O and Si–O bonds. [23,25]. The band 669.70–736.80 (s) cm⁻¹ of sodalite is near from the bands in the range 720–790 cm⁻¹ is associated with symmetric stretching vibration of 4-membered rings. (Fig. 4b). This band should be assigned to the 4-membered ring vibrations. Because these rings contain the lowest number of members of all rings occurring in the zeolite structure, therefore the bands due to these rings occur at relatively high wavenumbers in the pseudo lattice band range [26]. The band 1,644.28 (w), of sodalite, is near the bands at 1,647 and 1,648 cm (Lewis sites) region is assigned to the zeolitic water in the channels of zeolite [27]. The bands at spectra 3,446; 3,460; and 3,482 are attributed to the asymmetric stretching mode of molecular water coordinated to the edges of the zeolite channels [28,29] and the band 3,534.71

(b) cm⁻¹ of sodalite is near the bands that are attributed to the asymmetric stretching mode of molecular water coordinated to the edges of the zeolite channels [29]. The bands that located at the lowest wave numbers 466 and 377 cm⁻¹, are corresponding to the characteristic bending vibrations carried out in the 4-membered rings (Table 2) [30].

4.3. TGA of the synthesized zeolites

The thermal behavior of synthesized sodalite TGA and DTG in the air at a heating rate of 10°C min⁻¹ are shown in Fig. 5, while Table 3 gives the temperatures for various percentages weight loss. The synthesized product shows up to three dehydration steps (0%–8% weight loss). The first step is fast and ranges between 27°C and 152°C; which may be attributed to a loss of observed moisture and entrapped solvents. The second step is also a fast degradation between 153°C and 423°C. The third step is also fast between 423°C and 600°C. The position of these DTG peaks and the number of dehydration steps can be attributed to the different compensating cation-water binding energies. As well as to the different energy associated with the diffusion of the desorbed water through the porous structure of the synthesized product. TGA curves also, showed a small weight loss in the range 0%–2% starting at 72°C until 152°C which may

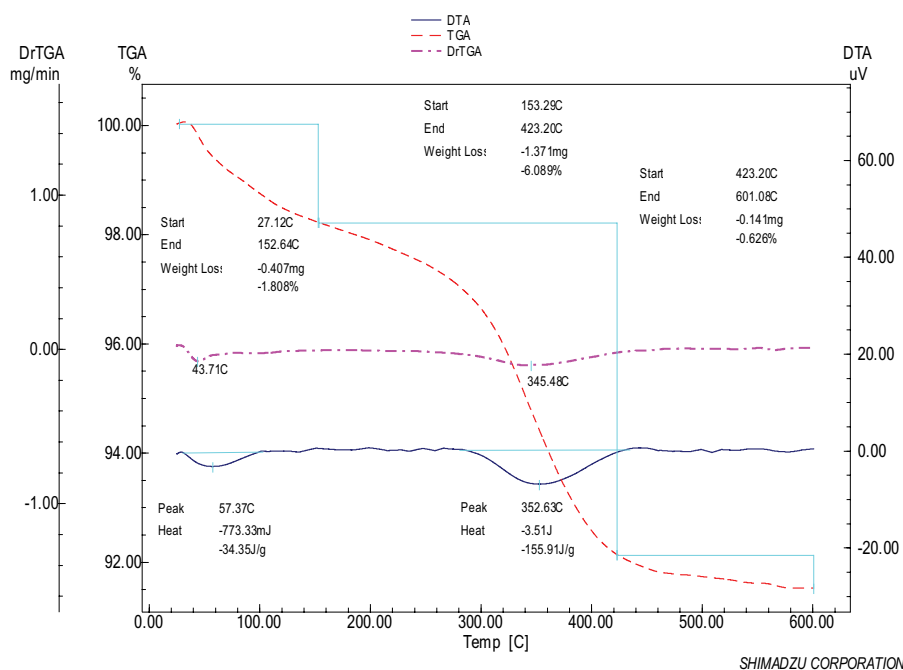


Fig. 5. Thermal analysis of the synthetic sodalite.

Table 3
Thermal analysis of the synthetic sodalite

| Type of zeolites | Temperature (°C) for various percentage decompositions* | | | |
|------------------|---------------------------------------------------------|-----|-----|-----|
| | 2% | 4% | 6% | 8% |
| Sodalite | 180 | 340 | 360 | 425 |

be attributed to a loss of observed moisture and entrapped solvents [31]. The thermographs of sodalite are given in Fig. 5.

5. Adsorptive properties of the synthetic sodalite

5.1. Batch adsorption studies

A batch adsorption experiment was conducted due to its simplicity in order to investigate the efficiency of the synthetic sodalite in reducing salinity as well as Na^{1+} ion. [32].

The experiments operated into natural groundwater samples from Wadi Qena which contaminated by salinity with concentrations up to 3,200 and 6,080 ppm and Na cation with concentration up to 1,320 ppm. The uptake of salinity and Na cation onto the synthetic zeolite as a function of their concentrations was studied at room temperature while keeping all other parameters constant with respect to dose.

5.2. Removal of salinity and Na^{1+} ion from groundwater samples at Wadi El-Assiuti

The concentration of salinity and Na^{1+} ion in some groundwater wells from Wadi El Assiuti are high (3,200–6,080 ppm and up to 1,320 ppm) respectively. The synthetic

zeolites (sodalite) was examined to reduce salinity as a function of their concentration by using varying TDS concentration from natural groundwater samples while keeping all other parameters constant. The time of the experiment was 1 h, at room temperature and pH of the solutions, the results are given in Table 4. While reducing, Na^{1+} ion by synthetic zeolite species was studied. at different pH from 4.5 to 10.5, the time between 1/12 h to 2, varying adsorbent dose (0.1, 0.2, 0.5, 1.0, and 1.5 g), and at a different temperature between 25°C and 50°C. The results in Table 4 indicate that the optimum conditions of salinity and Na^{1+} ion adsorption founded at pH 6–6.5 and time at 60 min.

The results in Table 4 indicate the efficiency of the synthetic zeolite (sodalite) in the reduction of salinity and Na^{1+} ion from groundwater samples. Based on the Si/Al ratios, this synthetic zeolite used is considered as low Si/Al ratios (<2) these types are possess an open cage within the lattice and a vast network of negatively charged open channels (accommodating Na^{1+} cation) due to presence of the common oxygen atom between Si and Al tetrahedral [33]. The pores or channels are of microscopically small size as of molecular dimensions and hence they are also called the “molecular sieves” which facilitate cation exchange in the adsorption process [34,35].

5.3. Factors effecting the Na^{1+} ion removal

The behavior of the synthetic (sodalite) toward the uptaking of Na^{1+} ion was studied as a function of adsorbent dosage, temperature, pH, and contact time.

5.3.1. Effect of dosage

The adsorbent mass in the solution affects the adsorption process since it determines the availability of active

Table 4
Salinity and Na⁺ ion removal (%) by the synthetic sodalite

| Salinity of samples (ppm) | Na ⁺ ion conc. (ppm) | Salinity removal (%) of samples | Na ⁺ ion removal (%) |
|---------------------------|---------------------------------|---------------------------------|---------------------------------|
| Before treatment (ppm) | | After treatment (ppm) | |
| 6,080 | 1,320 | 26 | 39 |
| 3,200 | 1,806 | 27.3 | 39.4 |
| 3,960 | 2,100 | 26.4 | 40 |
| 4,480 | 1,200 | 26.1 | 367 |

sites [36]. In order to establish the effect of the adsorbent dosage on removal of Na⁺ ion experiments at concentrations (1,320 ppm) was performed with adding varying adsorbent dose (0.1, 0.2, 0.5, 1.0, and 1.5 g) to 50 mL of the contaminated with fixing other parameters. The experiments were done at room temperature, constant pH of the solution (pH 8–9.5), and contact time (1 h). The results are given in Table 5 and Fig. 6.

With concern to Na⁺ ion the rate of removal increases rapidly as the dosage of the synthetic zeolites increases until 1 g of adsorbent dosage Fig. 6. This may be attributed to the fact that a large adsorbent amount reduces the unsaturation of the adsorption sites and correspondingly, the number of such sites per unit mass comedown. Decreasing the total surface area is increasing the diffusional path length, and both contribute to decreasing the amount of adsorbed per unit mass [37]. This comparatively led to decreasing adsorption with increasing adsorbent amount.

5.3.2. Effect of pH

Generally, the pH value is a significant parameter for metal ions removal by using zeolite as well as it can influence the characteristic of the exchangeable ions [38]. In order to establish the effect of pH on up taking of Na⁺ ion from groundwater samples, batch equilibrium studies at different pH values (6–6.5, 8–9, 9–9.5, and 10.5–11) were carried out. The pHs were adjusted using HCl (0.1 N) and NaOH (0.1 N). The experiments were done at a constant dose (0.5 g), room temperature, and 1 h as constant time. The results are given in Table 6 and Fig. 7.

The results indicate that the adsorption of Na⁺ ion reached the maximum at pH 6–6.5 and pH 10.5–11 (Fig. 7). This may be attributed to the fact that at low pH < 6–6.5 the adsorption percentage was low due to increasing of the positive charge density (protons) on the surface site, resulting in electrostatic repulsion between Na⁺ ion and the edge groups with positive charges (Si–OH)²⁺ on the surface. The loss in the removal capacity at lower pH can, therefore, be described to be as a result of the collapse of the zeolite structure. Electrostatic repulsion decreases with increasing pH because of the reduction of positive charge density on the edges, thus resulting in an increase in metal ion adsorption on the surface. While in an alkaline medium, pH > 7 the surface of zeolite becomes negatively charged [39]. So that the maximum adsorption of Na⁺ ion occurred at pH of 6–6.5 and at pH values higher than pH 9–9.5, which metal precipitation, occurred, and adsorbent capacity

Table 5
Results of different zeolite dosages on the removal of Na⁺ ion

| Na ⁺ ion concs. (ppm) before treatment | Zeolite dosage (g) | Na ⁺ ions removal (%) after treatment |
|---------------------------------------------------|--------------------|--------------------------------------------------|
| 1,320 | 0.1 | 2.8 |
| | 0.2 | 16 |
| | 0.5 | 39 |
| | 1 | 78 |
| | 1.5 | 66 |

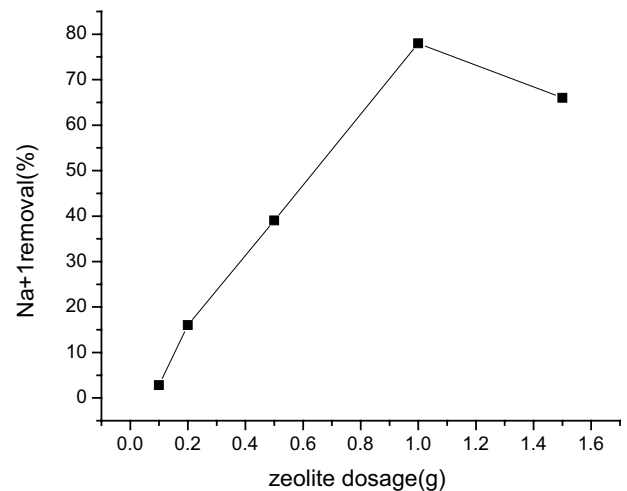


Fig. 6. Effect of different zeolite dosage on the removal (%) of Na⁺ ion.

Table 6
Results of pH changes on the removal of Na⁺ ion

| Na ⁺ ion conc. (ppm) before treatment | pH | Na ⁺ ion removal (%) after treatment |
|--------------------------------------------------|-------|-------------------------------------------------|
| 1,320 | 6–6.5 | 83 |
| | 8–9 | 41 |
| | 9–9.5 | 39 |
| | 10–11 | 78 |

decreases with an accumulation of metal ion. Finally, it was noted that an optimum pH of 6–6.5 was selected for further experiments.

5.3.3. Effect of temperature

The temperature has important effects on the adsorption process, whereas, an increase in temperature enhances the adsorption process. [40,41]. Usually, at elevated temperatures the cations uptakes increase due to increased affinity of the adsorbent (zeolite) for the metal and/or an increasing the active sites of the solid [42]. stated that, the energy of the system facilitates the attachment of metals on the zeolite surface at higher temperatures. Also, at higher temperatures ions become smaller due to their

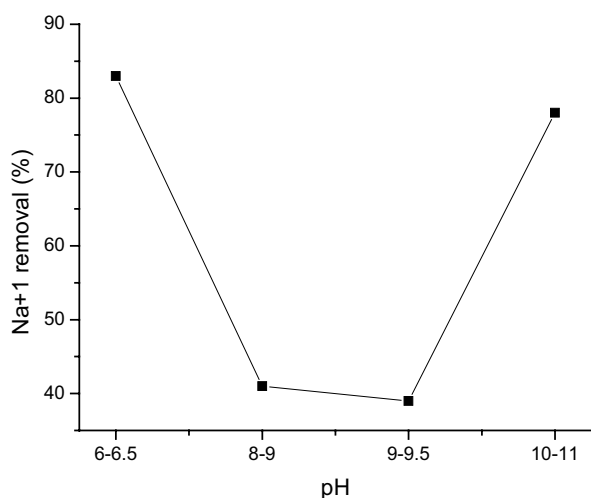


Fig. 7. pH vs. removal (%) of Na⁺ ion by the synthetic sodalite.

reduced hydration and their movement becomes faster resulting in higher removal efficiencies [43]. In order to establish the effect of temperature on the removal of Na⁺ ion from groundwater, experiments were carried out at different temperatures between 25°C and 50°C. With initial concentrations for Na⁺ ions are 1,320 ppm respectively and with constant the other factors as in the previous experiments. The results are given in Table 7 and Fig. 8.

The results showed that the adsorption rates of Na⁺ ion increase and reached the maximum at a temperature from 30°C to 40°C. With increasing temperature to more than 50°C the adsorption percent decreases. (Fig. 8). This may be due to change the equilibrium capacity of the adsorbent for adsorbate with increasing temperature to 40°C. At temperature >50°C, partial dissolution of the zeolite may be caused and led to decreasing the adsorption percent. This is given a production that the cations sorption onto the previous zeolites may be an exothermic process. [44].

5.3.4. Effect of contact time

The removal of Na⁺ ion from ground samples in the study area was studied as a function of contact time. The time range changes from 0 to 180 min at constant all other factors. The results are given in Table 8 and Fig. 9.

It is noted from Table 8 and Fig. 9 that removal percent of Na⁺ ion is increased with increasing time and reached the maximum at contact time 2 h. With increasing time >2 h, the ions up taking remain constant. This probably due to the saturation of the adsorbent surface area after 2 h. The optimum adsorbent dose and varying contact time, it is found that up to 2 h. And the maximum removal (%) of this ion is 81% by sodalite as shown in Table 8 and Fig. 9. For the further optimization of other parameters, the contact time was considered as the equilibrium time corresponding to the adsorbent and adsorbate [45,46].

5.4. Adsorption isotherms of Na⁺ ion by synthetic sodalite

The equilibrium adsorption of the Na⁺ ion was carried out by contacting 0.5 g of the previous synthetic zeolite with

Table 7
Results show the effect of temperature on the removal (%) of Na⁺ ion

| Na ⁺ ion conc. (ppm) before treatment | Temperature (C°) | Na ⁺ ion removal (%) after treatment |
|--------------------------------------------------|------------------|-------------------------------------------------|
| 1,320 | 20–25 | 40 |
| | 30–35 | 80 |
| | 35–40 | 82 |
| | 50–55 | 31 |

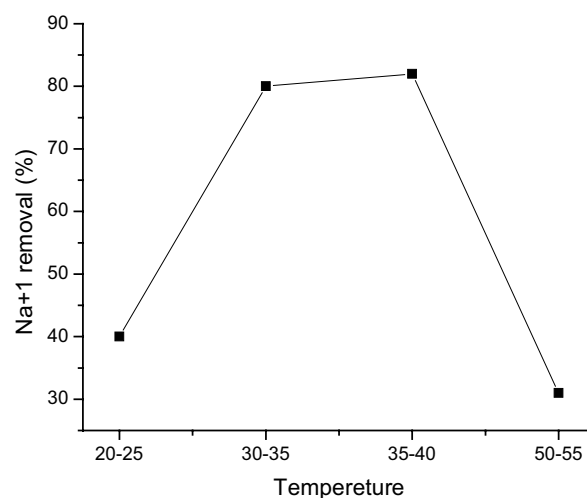


Fig. 8. Effect of temperature on adsorption of Na⁺ ion by the synthetic sodalite.

Table 8
Effect of contact time on the removal of Na⁺ ion

| Na ⁺ ion conc. (ppm) before treatment | Time (h) | Na ⁺ ion removal (%) after treatment |
|--------------------------------------------------|----------|-------------------------------------------------|
| 1,320 | 0 | 0 |
| | 1/2 | 30 |
| | 1 | 40 |
| | 2 | 81 |
| | 3 | 79 |

different concentrations 1,320; 1,806; 2,100; and 1,200 ppm from Na⁺ ion under room temperature, for 1 h and at pH 6–6.5 on the shaker. The mixture was filtered, and the filtrate analyzed for the metal ions concentration using AAS. And the data was fitted into the following isotherms: Langmuir and Freundlich [47].

5.5. Langmuir and Freundlich

Adsorption isotherm experiments were carried out by contacting 0.5 g of the synthetic zeolite with 50 mL of groundwater solution for Na ion treatment at a constant temperature, pH, and time. The results were fitted with Langmuir, Freundlich isotherm equations (Tables 9–11 and Fig. 10).

Based on the data given in Tables 9–11, the plots of $1/q_e$ vs. $1/C_e$ and $\log q_e$ vs. $\log C_e$ of Na^+ ion were depicted to show the Langmuir and Freundlich isotherms, respectively as shown in Fig. 10. The results proved that Langmuir

and Freundlich models were adopted to apply in the present study to isotherm modeling. Langmuir adsorption isotherm model is ($R^2 = 0.9$ for Na^+), the dimensionless constant of Langmuir isotherm is called equilibrium parameter (R_L). The values of R_L (Table 10) reflected the nature of the adsorption process. $R_L > 1$, $R_L = 1$, ($0 < R_L < 1$), and $R_L = 0$ for unfavorable adsorption, linear adsorption,

Table 9
Parameters calculated from Langmuir and Freundlich adsorption isotherms of Na^+ ion

| C_0 (mg/L) | C_e (mg/L) | q_e (mg/g) | Langmuir | | Freundlich | |
|-----------------|-----------------|-----------------|----------|---------|------------|------------|
| | | | $1/C_e$ | $1/q_e$ | $\log C_e$ | $\log q_e$ |
| 1,320 | 805 | 51.5 | 0.001 | 0.02 | 2.9 | 1.71 |
| 1,806 | 1,094 | 71.2 | 0.0009 | 0.014 | 3.04 | 1.85 |
| 2,100 | 1,260 | 84 | 0.0008 | 0.012 | 3.1 | 1.92 |
| 1,200 | 760 | 44 | 0.0013 | 0.023 | 2.88 | 1.6 |

Table 10
 R_L values for (Na^+) ion concentrations

| Na^+ ion concentration (ppm) | R_L value |
|---------------------------------------|-------------|
| 1,320 | 0.0007 |
| 1,806 | 0.0006 |
| 2,100 | 0.0005 |
| 1,200 | 0.0008 |

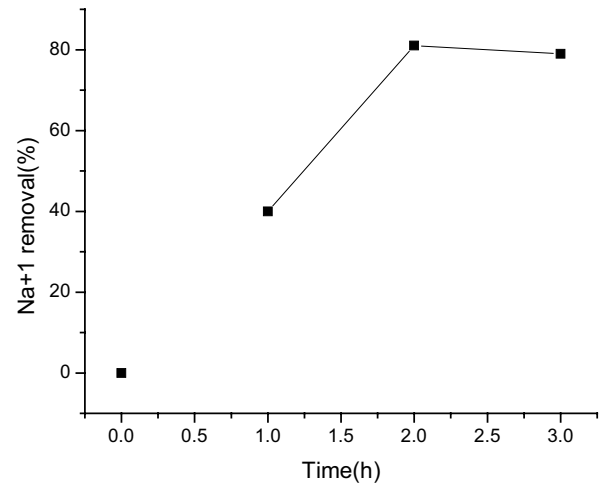


Fig. 9. Effect contact time on the removal of Na^+ ion by the synthetic sodalite.

Table 11
Linear regression equation's Langmuir and Freundlich isotherm and constants for adsorption of Na^+ ion by sodalite

| Metal ion | Langmuir | | | Langmuir equations |
|---------------|--------------|--------------|--------------|----------------------|
| | q_m (mg/g) | K_L (L/mg) | R^2 | |
| Na^+ | 0.6 | – | 0.7 | $Y = 0.66X$ |
| | Freundlich | | | Freundlich equations |
| | n | $1/n$ | K_f (mg/g) | R^2 |
| | 0.63 | 1.59 | – | 0.7 |

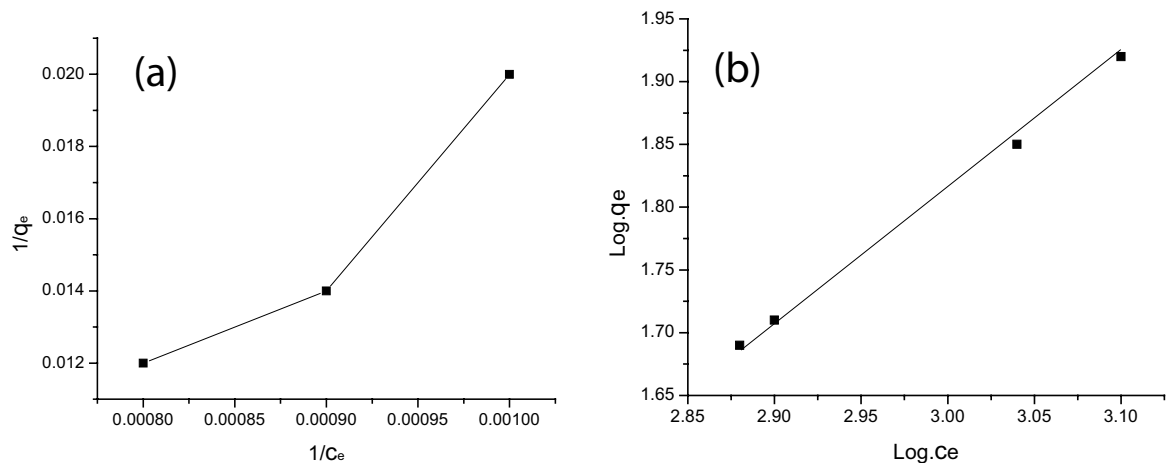


Fig. 10. Langmuir and Freundlich isotherm for Na^+ ion adsorption onto synthetic sodalite.

favorable adsorption, irreversible adsorption respectively [48,49]. The results are <1 indicates favorable adsorption. Freundlich adsorption isotherm is also adapted in the case of sodalite ($R^2 = 0.7$ for Na^+). Freundlich constants, K_f and n , calculated at from this investigation, for (Na^+) ion are 0 and 0.63, respectively for sodalite. Finally it is noted that value of $1/n$ for both (sodalite) is above one indicates cooperative adsorption [50].

6. Conclusion

The ground water samples that collected from Wadi El-Assiuti – Egypt wells were analyzed to determine the various physicochemical parameters such as salinity TDS, Na^+ ion. The results reveal that high concentration of salinity and Na^+ ion in some studied wells relative to (WHO 2004) and (A.R.E 2007). In this article, we could successfully synthesize sodalite from low-cost material natural clay materials (kaoline) and white sand using the fusion with NaOH method. The conditions of hydrothermal crystallization (zeolitization) were found to be at temperature of 170°C , and time span 72 h for raw material. The synthetic materials have been characterized by XRD, SEM, FT-IR, and DTA/TGA. The synthetic sodalite experiment is to determine the efficiency of the synthetic zeolites, in reducing a variety of salinity TDS with Na cation from ground water of Wadi El-Assiuti – Egypt. Batch experiments were carried out to investigate the effects of dosage of adsorbent, PH, temperature and time on both salinity and the Na^+ ion adsorption. The results showed that the synthetic sodalite has good efficiency in removal of salinity and the Na^+ ion with concentrations up to 6,000 and 1,320 ppm, respectively. The percent adsorption (%) was evaluated with changes in the parameters such as, dosage of adsorbent, PH and time for Na^+ ion. And it is found that the maximum removal ranged from 80%–82% for Na^+ ion at time 1 h, pH 10–11, at sodalite dose 10 g/L and temperature 35°C – 40°C , respectively. The Langmuir constants model for Na^+ ion sorption on the adsorption isotherms is fitted well. The R_L value in the present investigation at concentration more than 1,320 ppm was less than one, indicating that the adsorption of the metal ion by sodalite is favorable. Freundlich adsorption isotherm is also adapted in the case of sodalite ($R^2 = 0.7$) for Na^+ .

Acknowledgments

The authors are thankful to God. All supports providing from Sohag University and Assiut University and the chemistry administration for allowing the use of the laboratories.

References

- [1] J.E. Thomas, Fundamentos de Engenharia de Petróleo, E. Interciência, 2nd ed., São Paulo, SP, Brazil, 2004.
- [2] K.N. Jacob, A. John, U.S.N. Ibrahim, Groundwater quality and related water borne diseases in Dass town, Bauchi state, Nigeria, *J. Environ. Issues Agric. Dev. Countries*, 3 (2011) 2.
- [3] L.E. Apodaca, B.B. Jeffrey, C.S. Michelle, Water quality in shallow alluvial aquifers, Upper Colorado River Basin, Colorado, 1997, *J. Am. Water Resour. Assoc.*, 38 (2002) 133–143.
- [4] L. London, M.A. Dalvie, A. Nowicki, E. Cairncross, Approaches for regulating water in South Africa for the presence of pesticides, *Water SA*, 31 (2005) 53–60.
- [5] A. Bhatnagar, E. Kumar, M. Sillanpää, Nitrate removal from water by nano-alumina: characterization and sorption studies, *Chem. Eng. J.*, 163 (2010) 317–323.
- [6] M.A. Tofighy, T. Mohammadi, Nitrate removal from water using functionalized carbon nanotube sheets, *J. Hazard. Mater.*, 90 (2012) 1815–1822.
- [7] A. Santafé-Moros, J.M. Gozávez-Zafrilla, J. Lora-García, Performance of commercial nanofiltration membranes in the removal of nitrate ions, *Desalination*, 185 (2005) 281–287.
- [8] M.A. Saleh, E. Ewane, J. Jones, B.L. Wilson, Chemical evaluation of commercial bottled drinking water from Egypt, *J. Food Compos. Anal.*, 14 (2001) 127–152.
- [9] H.S. Ibrahim, T.S. Jamil, E.Z. Hegazy, Application of zeolite prepared from Egyptian kaolin for the removal of heavy metals: II. isotherm models, *J. Hazard. Mater.*, 182 (2010) 842–847.
- [10] Sh.V. Khachatryan, Heavy metal adsorption by Armenian natural zeolite from natural aqueous solutions, *J. Chem. Biol.*, 2 (2014) 31–35.
- [11] A. Borhade, A.G. Dholi, S.G. Wakchaure, Synthesis, characterization and crystal structure of gallosilicate perchlorate sodalite, *Int. J. Chem.*, 2 (2010).
- [12] M.M. Abd El-Ghani, Environmental correlates of species distribution in arid desert ecosystems of eastern Egypt, *J. Arid Environ.*, 38 (1998) 297–313.
- [13] A.A. Hassan, Habitat and Plant Species Diversity Along the Red Sea Coast in Egypt, M.Sc. Dissertation, Faculty Science, Cairo University, Egypt, 2003.
- [14] F.M. Salama, M.K. Ahmed, N.A. El-Tayeh, S.A. Hammad, Vegetation analysis, phenological patterns and chorological affinities in Wadi Qena, Eastern Desert, Egypt, *Afr. J. Ecol.*, 50 (2012) 193–204.
- [15] F.M. Salama, M.M. Abd El-Ghani, N.A. El-Tayeh, Vegetation and soil relationships in the inland wadi ecosystem of central Eastern Desert, Egypt, *Turk. J. Bot.*, 37 (2013) 489–498.
- [16] WHO, Nitrate and Nitrite in Drinking Water, Background Document for Development of WHO Guidelines for Drinking Water Quality, World Health Organization, WHO/SDE/WSH/07.01/16/Rev/1, 2007.
- [17] EHCW, Egyptian Standards for Drinking and Domestic Uses, Egyptian Higher Committee for Water, EHCW, Cairo, Egypt, 2014.
- [18] E. Safi, Guide to Preparation of Stock Standard Solutions, 1st ed., Chemiasoft, 2011.
- [19] W. Fan, K. Morozumi, R. Kimura, T. Yokoi, T. Okubo, Synthesis of nanometer-sized sodalite without adding organic additives, *Langmuir*, 24 (2008) 6952–6958.
- [20] C.A. Ríos, C.D. Williams, M.A. Fullen, Nucleation and growth history of zeolite LTA synthesized from kaolinite by two different methods, *Appl. Clay Sci.*, 42 (2009) 446–454.
- [21] F. Porcher, Y. Dusausoy, M. Souhassou, C. Lecomte, Epitaxial growth of zeolite X on zeolite A and twinning in zeolite A: structural and topological analysis, *Mineral. Mag.*, 64 (2000) 1–8.
- [22] I. Lapiques, L. Heller-Kallai, Reactions of met kaolinite with NaOH and colloidal silica—comparison of different samples (Part 2), *Appl. Clay Sci.*, 35 (2007) 94–98.
- [23] G.H. Li, FT-IR Studies of Zeolite Materials: Characterization and Environmental Applications, Ph.D. Thesis, Graduate College, The University of Iowa, Iowa City, 2005, pp. 162.
- [24] C.A. Ríos, C.D. Williams, Synthesis of zeolitic materials from natural clinker: a new alternative for recycling coal combustion by-products, *J. Fuel*, 87 (2008) 2482–2492.
- [25] A.A. Mohammed, I.K. Shakir, K.K. Esgair, The use of prepared zeolite Y from Iraqi kaolin for fluid catalytic cracking of vacuum gas oil, *J. Eng.*, 19 (2013) 1256–1270.
- [26] H. Wang, E.A. Turner, Y. Huang, Investigations of the adsorption of *n*-pentane in several representative zeolites, *J. Phys. Chem. B*, 110 (2006) 8240–8249.
- [27] C. Blanco, F. Gonzalez, C. Pesquera, I. Benito, S. Mendioroz, J.A. Pajares, Differences between one aluminic palygorskite and

- another magnesian by infrared spectroscopy, *J. Spectrosc. Lett.*, 22 (1989) 659–673.
- [28] D. Zhao, J. Zhou, N. Liu, Preparation and characterization of Mingguang palygorskite supported with silver and copper for antibacterial behavior, *Appl. Clay Sci.*, 33 (2006) 161–170.
- [29] H. Faghihian, N. Godazandeha, Synthesis of nano crystalline zeolite Y from bentonite, *J. Porous Mater.*, 16 (2009) 331–335.
- [30] W. Mozgawa, T. Bajda, Spectroscopic study of heavy metals sorption on clinoptilolite, *Phys. Chem. Miner.*, 31 (2005) 706–713.
- [31] C. Covarrubias, R. Garcia, R. Arriagada, J. Yanez, T. Garland, Cr(III) exchange on zeolites obtained from kaolin and natural mordenite, *Microporous Mesoporous Mater.*, 88 (2006) 220–231.
- [32] OECD, OECD Guidelines for the Testing of Chemicals, Organization for Economic Co-operation and Development Publications, Paris, 2000.
- [33] G. Mendoza, J. Gustavo, Synthesis and Applications of Low Silica Zeolites from Bolivian Clay and Diatomaceous Earth, Chemical Technology, Department of Civil, Environmental and Natural Resources Engineering, Lulea University of Technology, Sweden, 2017.
- [34] Okorie, A. Julie, Fabrication and Characterization of Zeolites and its Application in Heavy Metal Capture, 2016.
- [35] Y. Ping, Use of Natural Zeolites in the Recovery of Metals, Central Ostrobothnia University of Applied Sciences Press, Kokkola, 2010, pp. 5–18.
- [36] A.A. Ismail, R.M. Mohamed, I.A. Ibrahim, G. Kini, B. Koopman, Synthesis, optimization and characterization of zeolite A and its ion-exchange properties, *Colloids Surf., A*, 366 (2010) 80–87.
- [37] A. Shukla, Y.-H. Zhang, P. Dubey, J.L. Margrave, S.S. Shukla, The role of sawdust in the removal of unwanted materials from water, *J. Hazard. Mater.*, 35 (2002) 137–152.
- [38] S.K. Ouki, M. Kavannagh, Treatment of metals-contaminated wastewaters by use of natural zeolites, *Water Sci. Technol.*, 39 (1999) 115–122.
- [39] M.W. Munthali, E. Johan, N. Matsue, Proton adsorption selectivity of zeolites in aqueous media: effect of exchangeable cation species of zeolites, *Environments*, 2 (2015) 91–104.
- [40] S. Çoruh, O.N. Ergun, Ni²⁺ removal from aqueous solutions using conditioned clinoptilolites: kinetic and isotherm studies, *J. Environ. Prog. Sustainable Energy*, 28 (2009) 162–172.
- [41] A.S. Sheta, A.M. Falatah, M.S. Al-Sewailem, E.M. Khaled, A.S.H. Sallam, Sorption characteristics of zinc and iron by natural zeolite and bentonite, *Microporous Mesoporous Mater.*, 61 (2003) 127–136.
- [42] V.O. Arief., K. Trilestari, J. Sunarso, N. Indraswati, S. Ismadji, Recent progress on biosorption of heavy metals from liquids using low-cost biosorbents: characterization, biosorption parameters and mechanism studies, *Clean Soil Air Water*, 36 (2008) 937–962.
- [43] V.J. Inglezakis, M.M. Loizidou, H.P. Grigoropoulou, Ion exchange studies on natural and modified zeolites and the concept of exchange site accessibility, *J. Colloid Interface Sci.*, 275 (2004) 570–576.
- [44] S. Chatterjee, Mw. Lee, Ds. Lee, Sh. Woo, Nitrate removal from aqueous solutions by cross-linked chitosan beads conditioned with sodium bisulfate, *J. Hazard. Mater.*, 166 (2009) 508–513.
- [45] Mall and Upadhyay, (1998); Ho and McKay, 13(2003) 228.
- [46] N.Y. Mezenner A. Bensmaili, Kinetics and thermodynamic study of phosphate adsorption on iron hydroxide-egg shell waste, *Chem. Eng. J.*, 147 (2009) 87–96.
- [47] E. Erdem, N. Karapinar, R. Donat, The removal of heavy metal cations by natural zeolites, *J. Colloid Interface Sci.*, 280 (2004) 309–314.
- [48] N. Ünlü, M. Ersoz, Adsorption characteristics of heavy metal ions onto a low-cost biopolymeric sorbent from aqueous solutions, *J. Hazard. Mater.*, 136 (2006) 272–280.
- [49] C. Zhang, R.P. Lively, K. Zhang, J.R. Johnson, O. Karvan, W. Koros, Unexpected molecular sieving properties of zeolitic imidazolate framework-8, *J. Phys. Chem. Lett.*, 3 (2012) 2130–2134.
- [50] A.A. Chabanim, A. Bensmaili, Kinetic modeling of the adsorption of nitrates by ion exchange resin, *Chem. Eng.*, 125 (2006) 111–117.